

# Co(II) Schiff base complex decorated on polysalicylaldehyde as an efficient, selective, heterogeneous and reusable catalyst for epoxidation of olefins in mild and self-coreductant conditions

Milad Kazemnejadi<sup>1</sup> · Alireza Shakeri<sup>2</sup> · Mahsa Nikookar<sup>1</sup> ·  
Mohammad Mohammadi<sup>1</sup> · Mohsen Esmailpour<sup>3</sup>

Received: 3 April 2017 / Accepted: 26 June 2017 / Published online: 10 July 2017  
© Springer Science+Business Media B.V. 2017

**Abstract** A new Co(II)-Schiff base complex was decorated on a polysalicylaldehyde (PSA) framework and used as a selective and efficient catalyst for the epoxidation of alkenes in the presence of O<sub>2</sub> as a green source of oxygen without aco-reductant. The catalyst was characterized step by step by FTIR, UV–Vis, <sup>1</sup>H NMR, TGA, CHN, XPS and EDX analyses. Loading an amount of Co ions in the catalyst as well as its leaching amount were studied by an ICP-OES instrument. The catalyst demonstrated excellent activity for the of a variety of alkenes in a mild, inexpensive and efficient protocol. Also, the catalyst can be simply recovered from the reaction mixture and reused for several times without any noticeable loss in its activity. Reaction parameters including temperature, oxygen flow volume, catalyst amount and solvent were screened by reaction time. Catalytic studies including XPS spectroscopy and some blank experiments were performed to obtain an initial insight into the reaction mechanism. Also, the reactivity of the novel catalyst was evaluated as the turnover frequency.

---

**Electronic supplementary material** The online version of this article (doi:[10.1007/s11164-017-3027-z](https://doi.org/10.1007/s11164-017-3027-z)) contains supplementary material, which is available to authorized users.

---

✉ Milad Kazemnejadi  
miladkazemnejad@yahoo.com

✉ Mohsen Esmailpour  
m1250m551085@yahoo.com

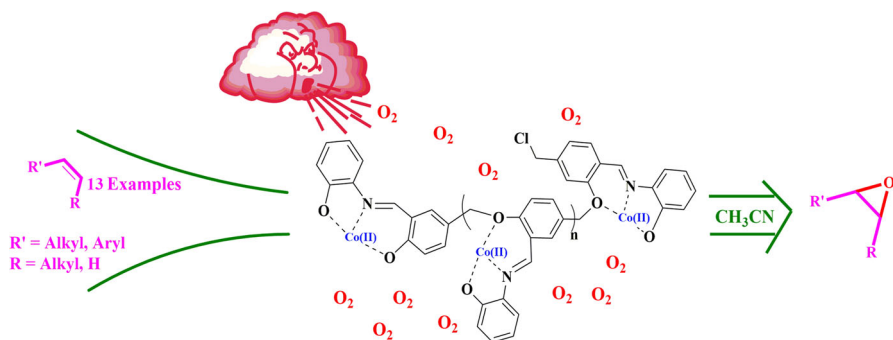
Alireza Shakeri  
Alireza.shakeri@khayam.ut.ac.ir

<sup>1</sup> Department of Chemistry, College of Sciences, Golestan University, Gorgan, Iran

<sup>2</sup> Faculty of Chemistry, University College of Science, University of Tehran, Tehran, Iran

<sup>3</sup> Department of Chemistry, College of Sciences, Shiraz University, Shiraz 71946 84795, Iran

**Graphical Abstract** A new and efficient protocol have been developed for the selective epoxidation of olefins using a heterogeneous recyclable Co(II)-Schiff base complex of polysalicylaldehyde in mild and self-coreductant conditions by molecular oxygen.



**Keywords** Epoxidation · Polysalicylaldehyde · Self-coreductant · Solid support · Co-polymeric Schiff base complexes

## Introduction

Due to the high reactivity of epoxides, they can be used as useful intermediates, building blocks and precursors in different industries as well as in organic synthesis [1, 2]. Epoxide derivatives have been largely used in surfactants, paints, and epoxy resins and have the potential for the production of bulk materials [3]. Epoxidation of alkenes is one of the most important and applicable reactions in organic synthesis [4]. So, finding suitable catalytic systems to provide desirable amounts of conversion and selectivity seems necessary [5]. The Mukaiyama reaction is a general method for the aerobic epoxidation of olefins by metal catalysts in the presence of an aldehyde [6]. Also, Halcon–Acro and Sumitomo processes have been used for the epoxidation of alkenes [5], but these methods have different by-products.

Various homogeneous and heterogeneous catalysts have been reported for the epoxidation of alkene in the presence of molecular oxygen as an inexpensive and safe oxidant compared to peroxides [7–12]. Due to the ability of homogeneous catalysts in reversible oxygen bonding and also their high activities, they have attracted significant attention for the oxidation of alkenes [13–15], but, in a homogeneous reaction, the isolation of the products and the reuse of the catalyst after the reaction become difficult [16]. Recently, attention has been focused on metal–Schiff base complexes for aerobic oxidation of olefins [17]. A diversity of transition metal complexes have been used as heterogeneous catalysts for alkene epoxidation [18], including Au, Ti [19], Fe/V [20, 21], Mn [22, 23], Ni [24], Yb [25] and W [26]. Co complexes are known as efficient catalysis for the epoxidation of

olefins [27], and the potential of Co complexes for the aerobic epoxidation of olefins has been known for decades [28]. Previously, Salavati-Niasari et al. [29] have reported the epoxidation of olefins by Co-Schiff base complex-supported MWCNTs.

Lately, Hu et al. [30] have shown the catalytic activity of  $\text{Co}(\text{OAc})_2$  in ionic liquid with hydrogen peroxide. Various heterogeneous Co-catalysts have been reported for the successful aerobic epoxidation of olefins, including: the cobalt-based metal-organic framework STA-12 [31], Co-substituted zeolite [32],  $\text{CoAlPO-36}$  [33],  $\text{CoOx-MCM-41}$  [34], cobalt complexes immobilized on HMS modified by organic amines [35], Co-hydroxyapatite [36], and so on [37]. Immobilization of Co complexes on solid polymer supports is another strategy for the preparation of heterogeneous catalysts that address some technical and economical obstacles [38]. Most recently, much attention has been paid to this strategy in order to catalyze various types of reactions [39]. Some reports showed higher epoxidation selectivity for polymer-supported metals than unsupported methods [40]. Nevertheless, not much has so far been reported for the use of polymer-bounded cobalt complexes for the epoxidation of olefins [41], among which are: (1) Co complex immobilized on polyaniline which selectively epoxidized *N*-cinnamoyl amino acid in the presence of molecular  $\text{O}_2$  and 2-methylpropanal [42], (2) silica-supported Co carboxylate [43], (3) polybenzimidazole-supported Co salt [44], and (4) Co complex supported on conductive polymer [45]. Previously, Kowalski et al. used cobalt-supported polyaniline, poly-*o*-toluidine, and poly-*o*-anisidine as heterogeneous efficient catalysts for the epoxidation of trans-stilbene [46]. Recently, a polyoxometalate-based framework has been developed by Haddadi et al. [3] as a heterogeneous catalyst for the epoxidation of alkene with aqueous  $\text{H}_2\text{O}_2$  in acetonitrile. Their system also showed higher catalytic activity for heterogeneous catalysts compared to corresponding homogeneous catalysts.

Due to environmentally benign and cost-effective aspects, the aerobic epoxidation of olefins without using co-reductants has attracted a large volume of attention from scientists and, from this point of view, cobalt-based catalysts showed a better performance among the other transition metals [47–49]. The Co-reductant is usually used as an oxygen acceptor in order to achieve satisfactory yields and selectivity [36]. First, free co-reductant Co-catalyst aerobic epoxidation of olefins was reported by Tang et al. [50] through introducing  $\text{Co}^{2+}$  into zeolite. Epoxidation of alkenes with free co-reductants has also been reported with Fe [51] and Ru [52, 53]. A sacrificial reductant mixed with  $\text{O}_2$  such as  $\text{H}_2$  [54], Zn powder [55] and  $\text{N}_2\text{O}$  [56, 57] have been other attempts for the environmental epoxidation of alkenes. However, due to environmental, safety, and economic considerations, the utilization of molecular oxygen alone for a catalytic epoxidation is more desirable.

Most of the mentioned methods for the aerobic epoxidation of olefins suffer from a lack of selectivity, the need for toxic materials as co-reductant (aldehydes, acetals, and  $\beta$ -ketoesters), toxic solvents, toxic and harmful peroxides, long reaction times and unsatisfactory yields. Therefore, the development of a new catalytic system to overcome these shortcomings and fulfill the criteria of a mild and efficient protocol for the epoxidation of olefins is still necessary. Salicylaldehyde is a safe, readily available organic compound from a health and reactivity point of view and can be

extracted from natural sources such as buckwheat [58]. Also, salicylaldehyde is known as one of the constituents of beaver Castoreum (Fig. 1) [59]. In the present work, we synthesized polysalicylaldehyde by self-polycondensation reaction of 2-hydroxy-5-chloromethyl-benzaldehyde, and then designed a polymer-Co complex through complexation of a Schiff base ligand on polysalicylaldehyde chains to Co(II) metals as a new heterogeneous, low-cost polymeric catalyst for the epoxidation of different alkenes in the presence of molecular oxygen as a green oxidant and acetonitrile as a solvent.

## Experimental

### Materials and instrumentation

All materials were purchased from Sigma Aldrich and Merck and used as received without any purification. FT-IR spectra were obtained using a Bruker Equinox 55 FT-IR spectrophotometer using KBr pellets. The  $^1\text{H-NMR}$  spectra were recorded on a Bruker Avance DPX 250 MHz spectrometer in  $\text{DMSO-}d_6$  using tetramethylsilane (TMS) as an internal reference. Elemental analyses (C, H, N) were performed on a Perkin Elmer-2004 instrument. UV-Vis analyses were performed on a UV Spectrolab BEL photonics. Thermal studies were performed on a NETZSCH STA 409 PC/PG in a nitrogen atmosphere with a heating rate of  $20\text{ }^\circ\text{C}/\text{min}$  in the temperature range of  $25\text{--}750\text{ }^\circ\text{C}$ . ICP analysis was performed by a VARIAN VISTA-PRO CCD simultaneous ICP OES instrument. Gel permeation chromatography (GPC) was acquired by a Knauer advanced scientific instrument (Germany), with a RI detector (Smartline 2300) PL gel  $10\text{ }\mu\text{m}$ ,  $10\text{E}3\text{ A}^\circ$  column. Monodispersed poly(methyl methacrylate), PMMA standards were used for calibration; the injected volume was  $20\text{ }\mu\text{L}$ . An Oxford INCA 350 energy-dispersive X-ray microanalysis system connected to the Hitachi S-4800 field emission scanning electron microscope was used for the energy dispersive X-ray spectrometry (EDX) measurement. The reaction progress was monitored by gas chromatography (GC). X-ray photoelectron spectroscopy (XPS) measurements were performed using an XR3E2 (VG Microtech) twin anode X-ray source with  $\text{AlK}\alpha = 1486.6\text{ eV}$ . GC analyses were recorded on a Shimadzu-14B gas chromatography instrument

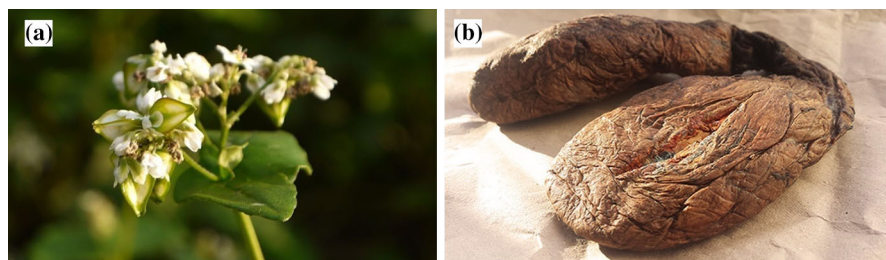
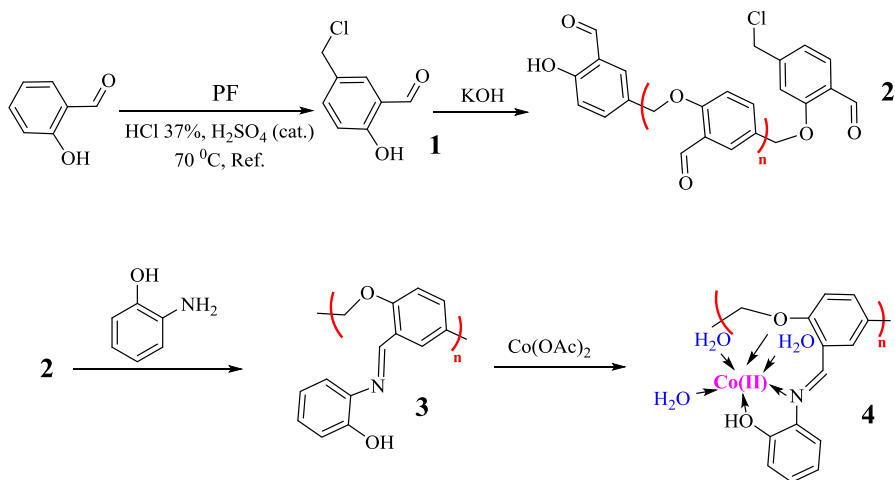


**Fig. 1** Images of buckwheat (a) and Castoreum (b)

equipped with a HP-1 capillary column (30 m, 0.25 mm, 0.25  $\mu\text{m}$ ) and  $\text{N}_2$  and anisole as carrier gas and internal standard, respectively.

### Preparation of PSA and PSA–Schiff base ligand

2-hydroxy-5-chloromethyl-benzaldehyde were synthesized and purified according to the previously described procedure [60]; salicylaldehyde (10 mmol), paraformaldehyde (0.49 g, 16.4 mmol) and HCl 37% (80 mmol) along with several drops of concentrated  $\text{H}_2\text{SO}_4$  as a catalyst were mixed together at 70  $^\circ\text{C}$  and stirred for 20 h (Scheme 1). The reaction mixture was cooled to room temperature and then water (20 mL) was added to the mixture and the product was extracted into  $\text{CH}_2\text{Cl}_2$  (20 mL). Some anhydrous  $\text{Na}_2\text{SO}_4$  was used for drying the organic phase. The  $\text{CH}_2\text{Cl}_2$  was removed with a rotary evaporator and the thick purple oil was set aside overnight, solidified upon standing and was isolated as a powder (9.5 mmol, 95% yield). Polymerization of 2-hydroxy 4-chloromethyl benzaldehyde **1** (Scheme 1) (6 mmol), was performed in the presence of concentrated KOH (50%, 20 mmol) at 80  $^\circ\text{C}$  which, after 16 h stirring, produced a dark yellow solid (PSA). This was filtered and washed with distilled water ( $3 \times 10$  mL) in order to completely eliminate acid and inorganic salts impurities (including KOH and KCl which can be formed during the polycondensation reaction with the release of HCl molecules) and placed in an oven (50  $^\circ\text{C}$ ) overnight. The final mass for **2** was 0.83 g (m.p. > 400  $^\circ\text{C}$ ). PSA (2 g, Mw  $\sim$  2190) along with 2-aminophenol (6 mmol) were added to 20 mL of ethanol. The reaction was stirred at room temperature for 12 h until a pale orange product was obtained which shows the formation of the Schiff base. The product was filtered, washed with methanol ( $2 \times 5$  mL) and isolated (1.6 g) after drying in an oven (50  $^\circ\text{C}$ ).



**Scheme 1** General scheme for preparation of the PSA–Schiff base–Co(II) complex **4** (proposed structure)

### Molecular weight studies of PSA

**Analytical method** The average molecular weight of the PSA was measured through acylation of the hydroxyl groups (end group analysis); an analytical method determined the hydroxyl number (%OH) by following Eq. (1) [61, 62]:

$$\%OH = \frac{(V_1 - V_2) \times f \times 0.0085 \times 100}{m_p} \quad (1)$$

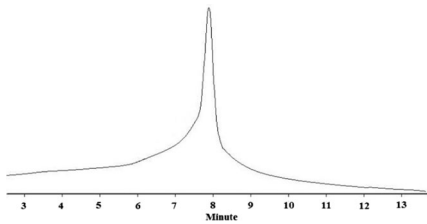
where  $V_1$  (mL) and  $V_2$  (mL) are the consumed volumes of potassium hydroxide required for titration of the blank and polymer samples, respectively,  $f$  is the coefficient of KOH solution 0.5 N thwhichat is equal to 0.732 [63], and finally  $m_p$  (g) is the mass of the polymer sample weighed for titration. The molecular weight obtained by this method will be the numerical molecular weight ( $\bar{M}_n$ ) which was measured by insertion of %OH into Eq. (2) [61, 62]:

$$\bar{M}_n = \frac{56.11 \times 1000}{\%OH} \quad (2)$$

To measure the hydroxyl number of the PSA, 0.017 g was weighed and dissolved in pyridine/acetic anhydride mixture (88:12) along with stirring at 50 °C for 8 h. One or two droplets of phenolphthalein indicator were added and the reaction mixture was then titrated with KOH (0.5 N). The hydroxyl number of the PSA was measured as 25.62 ( $V_2 - V_1 = 0.7$  mL, Eq. 1). So the  $\bar{M}_n$  was calculated by Eq. 2, equal to 2190 for PSA.

**GPC analysis** The molecular weight of the PSA was also studied with gel permeation chromatography (GPC). The results obtained from GPC are tabulated in Table 1. The numerical molecular weight obtained ( $\bar{M}_n$ ) by GPC was equal to 2226. Small differences (just 36 units) between the analytical and instrumentational measuring (GPC) for the numerical average molecular weight ( $\bar{M}_n$ ) of the PSA exhibited the accuracy of the methods as well as the obtained amount for  $\bar{M}_n$ . PSA has a well-polydisperse index (PDI = 1.43). An explanation for this low PDI was

**Table 1** Data obtained from GPC analysis of PSA

Types of molecular weight		
Weight average molecular weight	2278	
Numerical average molecular weight	2226	
Z average molecular weight	2328	
Z + 1 average molecular weight	2377	
Polydispersity index	1.430	
Peak molecular weight	2244	
Z average/weight average	1.028	
Z + 1 average/weight average	1.056	

the step-growth polymerization of 2-hydroxy-5-chloromethyl-benzaldehyde in alkali medium. The alkali medium neutralized the HCl molecules that were formed during the condensation reaction. This acts as a driving force for promoting the polymerization reaction and providing such a low PDI. The obtained molecular weight for the PSA clearly confirms the formation of PSA through polycondensation reaction.

### Complexation of Co to PSA–Schiff base ligand

The PSA–Schiff base Co(II) complex was prepared by the addition of ethanol (15 mL) to the PSA–Schiff base ligand (0.25 g) at 70 °C (underwent reflux). The reaction was stirred for 20 min, then Co(OAc)<sub>2</sub> (2.5 mmol) was added slowly to the mixture during 10 min. Stirring lasted for another 4 h. The brown sediments were filtered and washed with methanol (2 × 5 mL). The resultant product was placed in the oven overnight and then isolated as a brown powder (final isolated mass was 0.50 g).

Elemental analysis along with the color of the samples are shown in Table 2. The percentages of C and H of 2-hydroxy-5-chloromethyl-benzaldehyde clearly proved its formation. Due to polymerization, the percentage of C in the PSA was raised to 73.8%. The PSA–Schiff base ligand shows 5.84% for N which was the result of imine formation. Also, after the formation of the metal complexes, the C, H and N percentages reduced which demonstrated the insertion of Co in the PSA–Schiff base ligand. Table 2 shows the physical properties of the samples including their elemental analysis and colors.

### General procedure for catalytic epoxidation of alkenes

Epoxidation of olefins was carried out in a 25-mL three-necked round-bottom flask equipped with O<sub>2</sub> gas (as an oxidant) inlet (~1 atm., bubbling 15 mL/min), water condenser and magnet stirrer bar. In a typical run, a mixture of alkene (10 mmol) and 50 mg of catalyst **4** (2 mol%) were added to acetonitrile (20 mL) and the reaction was kept in a constant temperature oil bath at 60 °C. Molecular oxygen with a rate of 15 mL/min<sup>-1</sup> was bubbled during the reaction. The reaction mixture was stirred vigorously for a sufficient time. After completion of the reaction, the

**Table 2** Elemental analysis and colors of the compounds

Compounds	Color	Elemental analysis		
		%C	%H	%N
2-Hydroxy-5-chloromethyl-benzaldehyde	Purple	56.82 (56.33) <sup>a</sup>	4.25 (4.14) <sup>a</sup>	–
PSA	Yellow	70.11	4.35	–
PSA–Schiff base ligand	Orange	73.81	5.27	5.84
PSA–Schiff base Co(II) complex	Dark brown	65.27	3.31	7.02

<sup>a</sup> Theoretically calculated

catalyst was filtered off and the liquid organic product was quantified by GC. Also, the pure product was separated from the reaction mixture by silica-gel plate or silica-gel column chromatography, then their structures were identified by  $^1\text{H}$  NMR and  $^{13}\text{C}$  NMR spectra. Activity of the catalyst was expressed as the turnover frequency (TOF) and calculated from the moles of cyclohexene converted per mole of cobalt contained in the catalyst using the following equation:

$$\text{TOF} = \frac{\text{Moles (Converted cyclohexene)}}{\text{Moles of Co (Active site)} \times \text{Reaction time (h)}} \quad (3)$$

The conversion and selectivity of the cyclohexene epoxide were calculated by the following equations:

$$\text{Conversion (mol\%)} = \frac{(\text{Initial mol\%}) - (\text{Final mol\%})}{\text{Initial mol\%}} \times 100 \quad (4)$$

$$\text{Cyclohexene epoxide selectivity} = \frac{\text{GC peak area of cyclohexene epoxide}}{\text{GC peak area of all products}} \times 100 \quad (5)$$

The recovered catalyst which was obtained by simple filtration was washed with acetone ( $2 \times 10$  mL), dried at  $50$  °C for 1 h and then reused for the next run in the same conditions.

## Results and discussion

### Characterization of PSA and catalyst

#### FTIR spectra

Figure 2 shows the FTIR spectra of the samples. A new peak which appeared at  $1481\text{ cm}^{-1}$  in the spectrum of 2-hydroxy-5-chloromethyl-benzaldehyde **1** was attributed to the bending vibration of the methylene groups ( $-\text{CH}_2-$ ) (Fig. 2a). Another characteristic peak for **1** was  $725\text{ cm}^{-1}$  for the vibration of C–Cl, which demonstrated successful formation of the chloromethylene substitution on the salicylaldehyde. After polymerization of **1**, the stretching vibration of C–Cl in all the spectra at  $\sim 760\text{ cm}^{-1}$  showed the presence of the chloromethylene group in the terminal of the PSA chains (Fig. 2b). Moreover, the spectra showed C–H bending vibrations at  $1400$ – $1480\text{ cm}^{-1}$  for the chloromethylene group and confirmed the introduction of a  $-\text{CH}_2\text{Cl}$  group at the *para*-position compared with the hydroxyl group. Aromatic and aliphatic stretching vibrations of C–H can be seen in all the spectra in the ranges of  $\sim 3030$  to  $3710$  and  $\sim 2746$  to  $3000\text{ cm}^{-1}$ , respectively. The changes in the stretching vibration of the hydroxyl groups in the samples gives useful information about the structure of the samples. Due to the intense polymerization of the salicylaldehyde, the stretching vibration of hydroxyl groups at  $3200\text{ cm}^{-1}$  has been largely reduced (Fig. 2, dotted circle). Formation of the



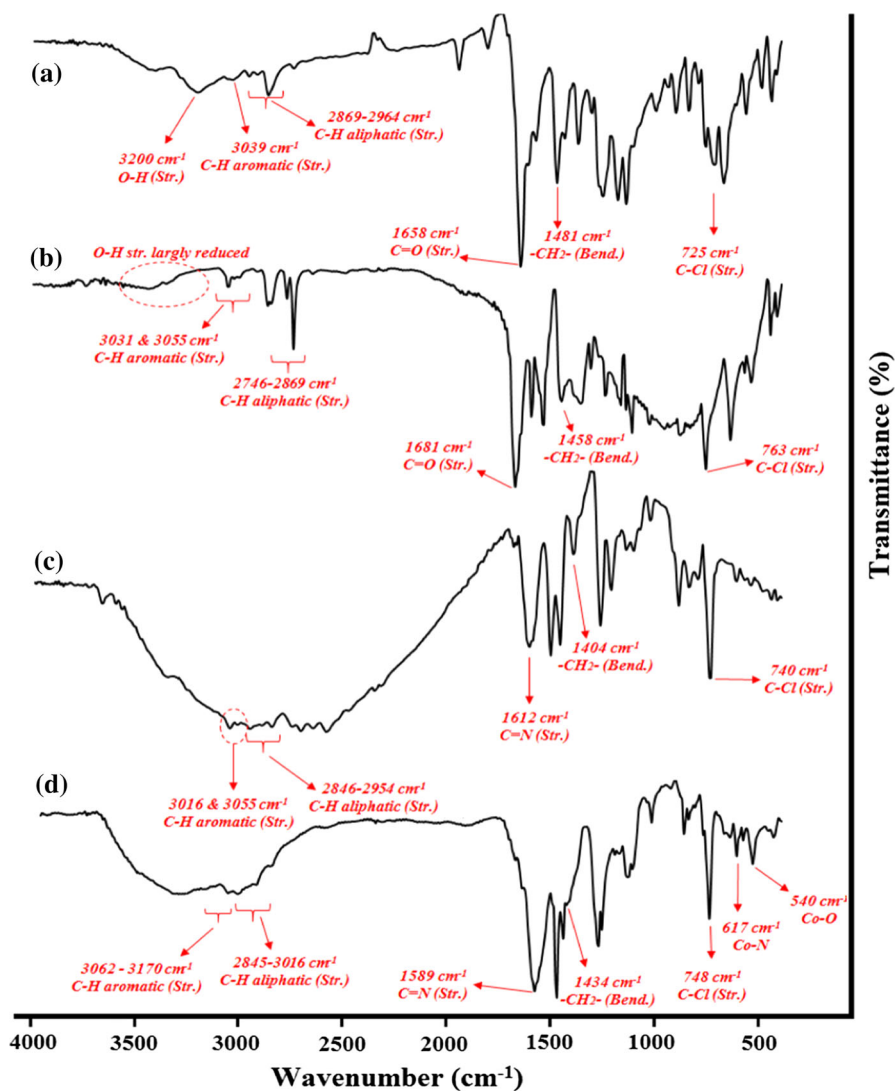


**Fig. 2** FTIR spectrum of *a* 2-hydroxy-5-chloromethyl-benzaldehyde **1**, *b* PSA **2**, *c* PSA-Schiff base ligand **3** and *d* PSA-Schiff base Co(II) complex **4**

Schiff base moiety on the PSA in the spectrum of the PSA-Schiff base ligand (Fig. 2c) provided a broad peak at  $3200\text{--}3300 \text{ cm}^{-1}$  representing the O-H phenolic groups with H-bonding.

The main characteristic peak for the PSA-Schiff base ligand was  $1612 \text{ cm}^{-1}$  related to the vibration of the Schiff base (C=N) bond which corroborated the imine formation. Coordination of Co(II) to N and O atoms in the PSA-Schiff base ligand causes the shift of C=N stretching vibrations to lower wavenumbers at  $1589 \text{ cm}^{-1}$  (Fig. 2d) [14]. Vibrations corresponding to Co-O and Co-N were found at 540 and

617  $\text{cm}^{-1}$ , respectively [52, 64]. Furthermore, this chelation reduced the intensity of the hydroxyl stretching vibration (greatly eliminating the H-bonding) at catalyst **4** and illustrated that chelation of Co metals also occurs through oxygen atoms (Fig. 2d).

### *<sup>1</sup>H NMR spectroscopic studies*

2-Hydroxy-5-chloromethyl-benzaldehyde **1** has been previously synthesized and, due to the presence of two directing groups on the phenyl, the chloromethylene group substituted at the *para*-position hydroxy group [65]. <sup>1</sup>H NMR of 2-hydroxy-5-chloromethyl-benzaldehyde **1** and PSA are shown in Fig. 3. Resonance for methylene protons was found at 4.58 ppm. Chemical shifts for aldehyde and hydroxyl protons for **1** were found at 9.88 and 11.06 ppm, respectively (Fig. 3a).

Methylene protons for PSA **2** are represented with three peaks at 4.09, 4.74 and 4.98 ppm (Fig. 3b). Aromatic protons were set in the region of 6.97–7.57 ppm for **1** and 7.11–8.33 ppm for PSA **2**. <sup>1</sup>H NMR spectrum of PSA shows two peaks for aldehyde at 10.22 and 10.41 ppm due to different chemical environments. Hydroxyl groups at terminal PSA chains exhibited a single peak at 11.33 ppm (Fig. 3b).

### *Electronic spectra*

The electronic spectra of the samples were scrolled in the region of 200–800 nm. Figure 4a shows UV–Vis spectra for the PSA, PSA–Schiff base ligand and PSA–Co(II) complex. A single peak at  $\sim 336$  nm with a shoulder at 296 nm in the electronic spectrum of PSA was assigned to  $\pi \rightarrow \pi^*$  and  $n \rightarrow \pi^*$  transitions related to the phenyl and carbonyl groups, respectively. The PSA–Schiff base ligand **3** exhibited three adsorption bands at 298, 356 and 444 nm [66, 67]. These adsorptions were due to  $n \rightarrow \pi^*$  and  $\pi \rightarrow \pi^*$ , resulting in the formation of an imine bond and also  $\pi \rightarrow \pi^*$  transitions for the benzene rings. The PSA–Schiff base Co(II) complex showed a broad peak at 440 nm resulting in  $d-d$  transitions for Co(II) [52]. Adsorption of  $\pi$  electrons related to the benzene rings appear as a shoulder at 374 nm for the catalyst **4** (Fig. 4a). UV–Vis spectra reported six-coordinated Co complexes and showed an absorption band at 400–500 nm which confirms that the coordination of Co in the catalyst **4** was six [52].

### *Thermal analysis*

Thermal studies of the PSA, PSA–Schiff base ligand and PSA–Schiff base Co(II) complex are shown in Fig. 4b. The spectra showed good thermal stability for all three samples. Thermal decomposition of PSA (Fig. 4b) occurs only in one step in the temperature span of 200–525 °C corresponding to a 47% weight loss. After that, the weight loss continues to 750 °C with a gentle slope which showed carbonization of the polymer. Advent of an additional weight loss step in the TGA curve of PSA–Schiff base ligand was attributed to the decomposition of the Schiff base moiety on the PSA chain and confirmed the Schiff base formation on the PSA. This decomposition occurs in the temperature range of 99–360 °C (8% weight loss). The

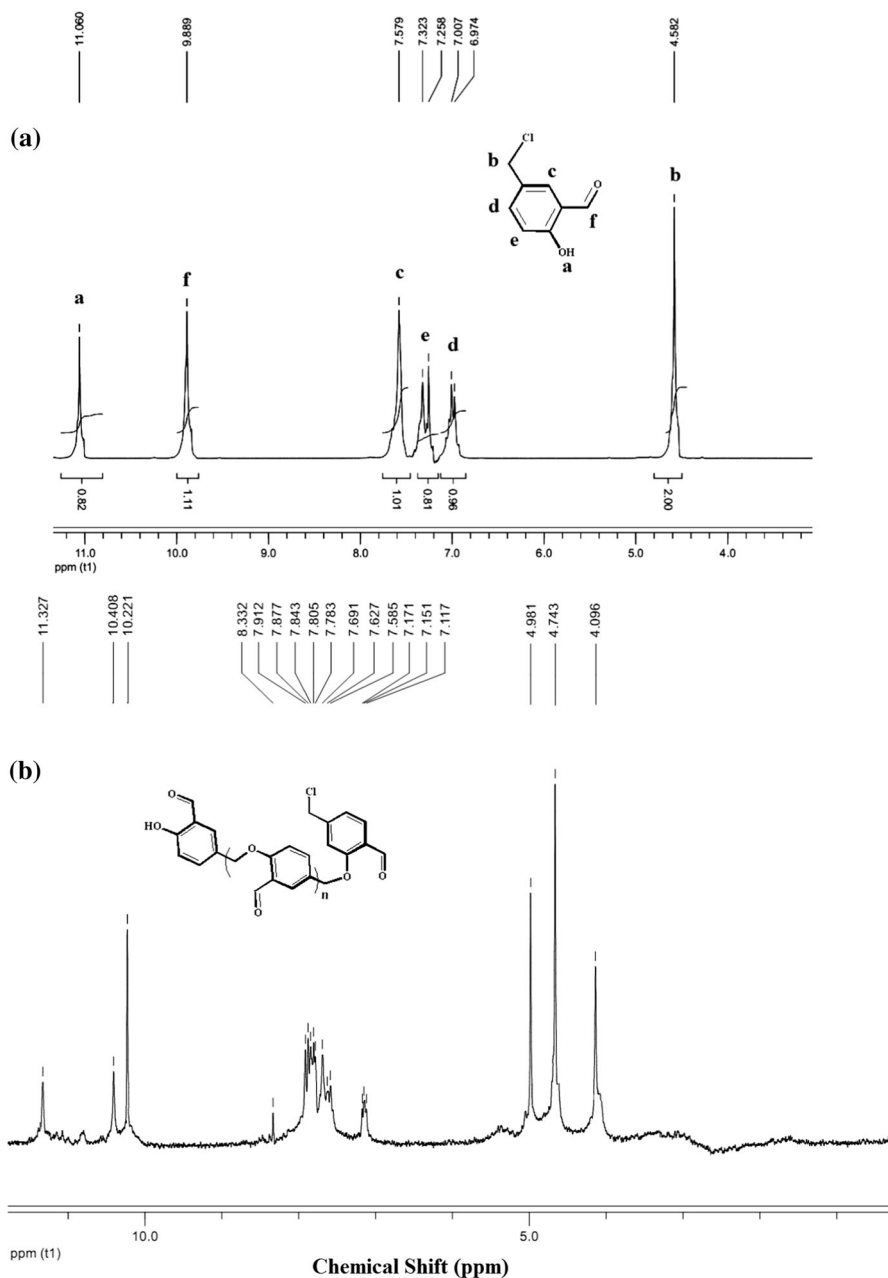


**Fig. 3**  $^1\text{H}$  NMR spectrum of *a* 2-hydroxy-5-chloromethyl-benzaldehyde **1** and *b* PSA **2**

second stage, which starts at 420 °C, shows decomposition of the PSA. Insertion of Co in the PSA–Schiff base ligand leads to about a 32% (300–500 °C) weight loss in the thermal spectrum of the PSA–Schiff base–Co(II) complex (Fig. 4b) in the first

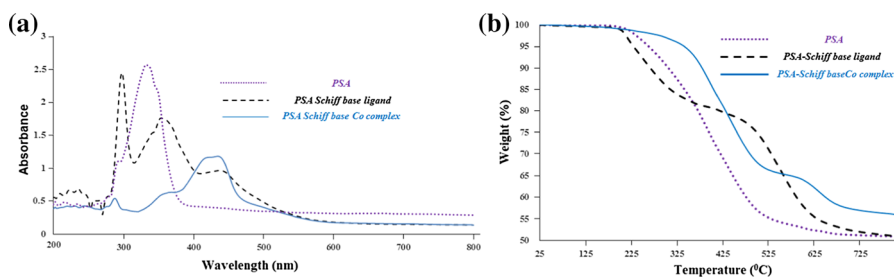


**Fig. 4** **a** UV-Vis spectra of PSA, PSA-Schiff base ligand and PSA-Schiff base Co(II) complex; **b** TGA analysis of PSA, PSA-Schiff base ligand and PSA-Schiff base Co(II) complex

stage. According to the thermal degradation of the Schiff base moiety in the PSA-Schiff base ligand, this amount was in accordance with the loading amount of Co obtained from inductive coupled plasma (ICP) analysis. The second step also belonged to PSA decomposition.

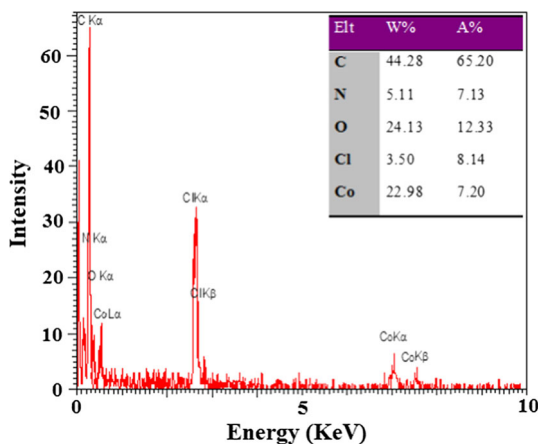
#### ICP measurement

The loading amount of Co on the PSA-Schiff base ligand was measured by ICP analysis. The experiments indicated that 23.57 mg (in 100 mg of catalyst) of Co was loaded on 100 mg of the PSA-Schiff base ligand framework.

#### EDX analysis

The elements of the catalyst **4** were detected by energy dispersive spectroscopy (EDX) analysis. Related information including intensity and weight of the elements are shown in the inset table of Fig. 5. The EDX spectrum clearly confirmed the Co complex formation on the PSA framework. Also, the spectrum shows the attendance of Cl atoms set at the end chains of the PSA framework.

**Fig. 5** EDX spectra of the PSA-Schiff base-Co complex



On the basis of the reported structure for the Co(II) complex by Refat et al. [52] along with the achieved results from FTIR, UV–Vis, TGA and EDX analyses, the most probable structure for catalyst **4** is shown at Scheme 1.

### Investigation of effective parameters for oxidation reactions

The influence of reaction parameters has been thoroughly investigated on the epoxidation of cyclohexene. The solvent, temperature, catalyst amount and molecular oxygen flow rate affected epoxide selectivity and conversion of the reactions and the corresponding results are shown in Fig. 6a–d. The solvent plays an important role in an epoxidation reaction [68]. High possible conversion (88%) and epoxide selectivity (89%) were achieved in acetonitrile as solvent. Other tested solvents (acetone, EtOH, MeOH, CHCl<sub>3</sub> and DCM) did not show a good performance compared to acetonitrile (Fig. 6a). Increasing the temperature to 60 °C enhanced the cyclohexene conversion, and the conversion increased almost proportionally with increasing temperature (Fig. 6b). No more conversion could be achieved at a temperature higher than 60 °C (Fig. 6b). The most epoxide selectivity was also obtained at 60 °C (88%) for 6 h. The chart in Fig. 6b (right) shows that the epoxide selectivity strongly depended on the temperature and that the catalyst did not have good selectivity at low temperatures. Also, the catalyst amount had an impressive role in the progress of the reaction (Fig. 6c). The reaction did not make any progress in the absence of the catalyst **4** (zero conversion, not shown in Fig. 6). Oxygen flow rate had the least effect on the reaction conversion and selectivity (Fig. 6d) among the other reaction parameters. This phenomenon demonstrates that the reaction rate was slower than the consumption of oxygen, proving that no large difference is seen between air and O<sub>2</sub> as oxidative agents. Above 15 mL/min, the O<sub>2</sub> flow rate had little influence on the epoxide selectivity. A flow rate of 15 mL/min of oxygen was sufficient to reach the highest possible conversion (Fig. 6d, 88%). Increasing the flow rate above 15 mL/min did not enhance the conversion.

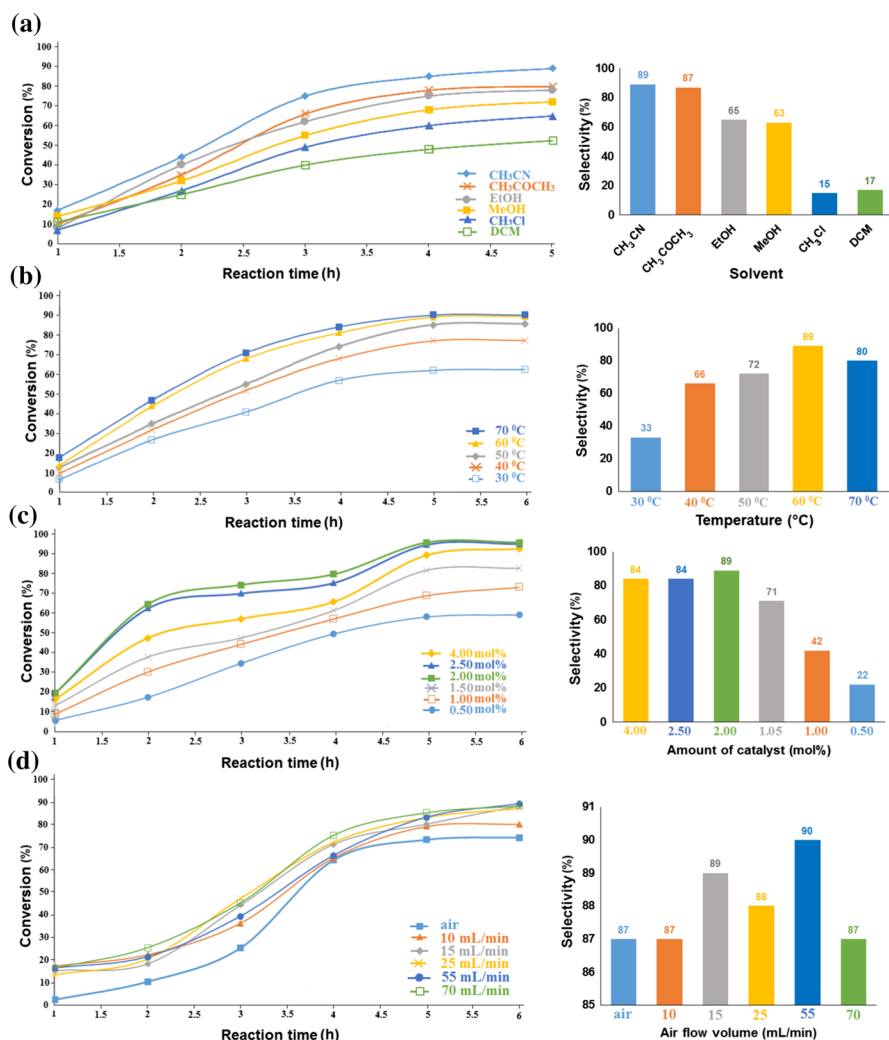
The reactions were performed in the absence of any aldehyde as coreductant. It is believed that the free aldehyde groups in the PSA framework in catalyst **4** play the role of co-reductant in the epoxidation of olefins.

TOF amounts for each effective parameter of the epoxidation reaction were also measured in order to measure the activity effect of the catalyst on temperature, solvent, molecular oxygen flow rate and catalyst amount in the reaction (Fig. 7). There was a good correlation between epoxide selectivity, percentage of conversion and TOF amounts in all cases. Optimization of each effective parameter causes the enhancement of TOF.

### Catalytic epoxidation of olefins

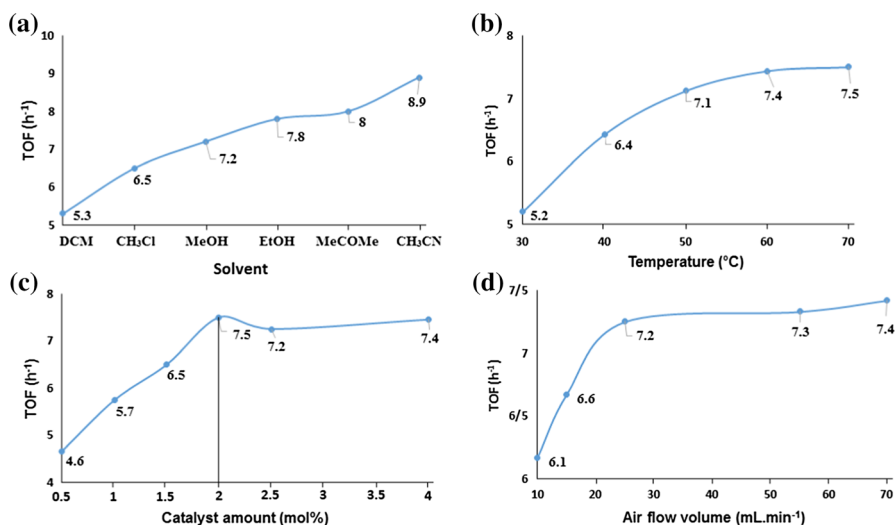
We then submitted various alkenes to the optimized reaction conditions: cyclohexene (10 mmol), catalyst **4** (50 mg, 2 mol%), acetonitrile (20 mL), O<sub>2</sub> (~1 atm., bubbling 15 mL/min), 60 °C, Time.

The catalytic activity of the PSA–Schiff base Co complex was investigated in the epoxidation of various types of olefins in O<sub>2</sub> atmosphere, and the corresponding



**Fig. 6** Influence of (a) solvent, (b) temperature, (c) catalyst amount and (d) air flow volume on conversion in the epoxidation of cyclohexene. The reaction selectivity corresponding to each parameter are depicted as *right column charts*. **a** Reaction conditions: cyclohexene (10 mmol), catalyst **4** (50 mg, 2 mol%), solvent (20 mL), O<sub>2</sub> (~1 atm., bubbling 15 mL/min), 60 °C, 5 h. **b** Reaction conditions: cyclohexene (10 mmol), catalyst **4** (50 mg, 2 mol%), solvent (20 mL), O<sub>2</sub> (~1 atm., bubbling 15 mL/min), temperature, 6 h. **c** Reaction conditions: cyclohexene (10 mmol), catalyst **4**, solvent (20 mL), O<sub>2</sub> (~1 atm., bubbling 15 mL/min), 60 °C, 6 h. **d** Reaction conditions: cyclohexene (10 mmol), catalyst **4** (50 mg, 2 mol%), solvent (20 mL), O<sub>2</sub> (~1 atm., bubbling 15 mL/min), 60 °C, 6 h

results are tabulated in Table 3. Among the endocyclic alkenes, cyclooctene with 92 and 98% conversion and selectivity, respectively, were the most reactive of all. This reactivity arises from the stability of cyclooctene as well as the high reactivity of its double bond [69]. Cyclohexene showed 89% epoxide selectivity. The potential of active allylic hydrogens to oxidation was responsible for reducing the epoxide

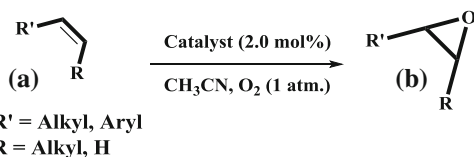


**Fig. 7** Calculated TOF amounts for the epoxidation of cyclohexene for **a** different solvents, **b** different temperatures, **c** various amounts of catalyst **4** and **d** various air flow volumes. For reaction conditions, see caption to Fig. 6

selectivity for cyclohexene. Open-chain alkenes such as styrene (Table 3, entry 1) and 1-octene (Table 3, entry 7) are epoxidized with moderate efficiency. The present method demonstrated low side reaction as shown for most of the entries in Table 3. Furthermore, catalyst **4** performed completely chemoselectively for the epoxidation of terminal alkene compared with the terminal  $\alpha,\beta$ -unsaturated terminal alkene demonstrated for 2-methylhexa-1,5-dien-3-one (Table 3, entry 12). Similarly, 1*H*-indene epoxidized with low efficiency (Table 3, entry 5). These results indicated that conjugated C=C bonds caused lower efficiencies compared to non-conjugated types. This property provided selectivity in the case of 2-methylhexa-1,5-dien-3-one (Table 3, entry 12) in which just terminal alkene was bearing the epoxidation. Chemoselectivity behavior of the catalyst **4** was also tested with substrates involving two C=C functional groups (Table 3, entries 10, 13). The method presented good selectivity toward the epoxidation of one equivalent C=C bond for the mentioned substrates. Also, high selectivity was achieved for the other substrates (Table 3). Steric hindrance on the C=C bond not only increased the reaction time but also decreased the conversion of the olefins such as 3,3-dimethylhex-1-ene (Table 3, entry 8) and 1-methoxy-2-methylprop-1-ene (Table 3, entry 11).

### Recycling study of the catalyst

It is well known that the advantages of a heterogeneous catalyst lie in the ease of recoverability, long-term stability, minimum leaching and minimum change in its activity [27]. Stability and recoverability of the catalyst were studied in the epoxidation of cyclohexene in the obtained optimum conditions. Figure 8 shows the

**Table 3** Oxidation of alcohols to carbonyl compounds

Entry	Alkene (a)	Product (b)	Time (h)	Conversion (%) <sup>a</sup>	Yield (%) <sup>b</sup>	Epoxide selectivity (%) <sup>a</sup>	TOF (h <sup>-1</sup> )
1			5.5	84	80	92	7.6
2			4.2	88	82	89	10.5
3			1.0	89	83	96	44.5
4			10.2	86	79	92	4.2
5			6.0	55	50	76	4.5
6			4.2	87	85	95	10.4
7			10.0	90	85	75	4.5
8			27.0	80	73	66	1.4
9			3.0	92	90	98	15.4
10			3.0	88	83	77	14.6
11			14.0	78	70	80	2.8
12			2.2	83	76	81	18.9
13			1.5	87	85	79	29.0

Reaction conditions: alkene (10 mmol), catalyst **4** (50 mg, 2 mol%), 60 °C, CH<sub>3</sub>CN (20 mL), O<sub>2</sub> (~1 atm. bubbling 15 mL/min), time

<sup>a</sup> GC analysis; using an internal standard technique (*Anisole*) and are based on alkenes

<sup>b</sup> Isolated yield

results obtained from the retrieval ability of the catalyst **4** including the leaching amount of the catalyst, conversion of cyclohexene and epoxidation selectivity. The catalyst was successfully recovered after completion of the reaction and characterized with FTIR spectra and reused for 5 runs without noticeable reactivity or selectivity loss. Also, amounts of metal leaching were measured by ICP analysis after every run. The results showed 3.5% cobalt leaching after the 5th run which corresponds to 80% cyclohexene conversion. Also, the experiments did not show



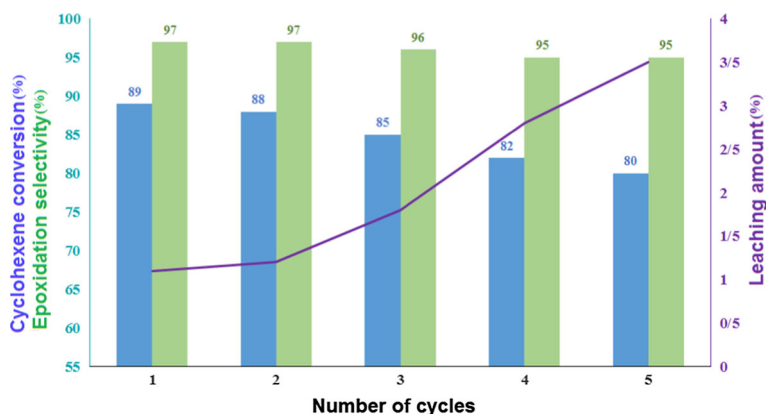


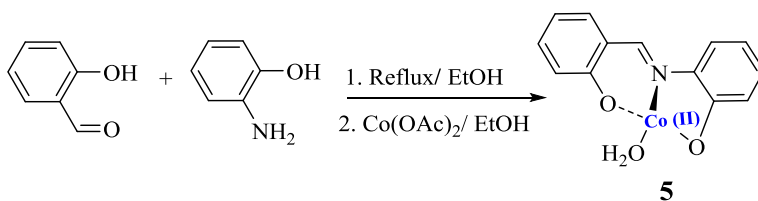
**Fig. 8** Conversion and selectivity percent as well as leaching amount percent of spent catalysis in reaction cycles. Reaction conditions: alkene (10 mmol), catalyst 4 (50 mg, 2 mol%), 60 °C, CH<sub>3</sub>CN (20 mL), O<sub>2</sub> (~1 atm, bubbling 15 mL/min), 4.2 h

any considerable drop of selectivity during the reaction cycles and just 2% loss occurred in selectivity after 5 runs. These data strongly confirm the stability and reactivity of the PSA–Schiff base–Co complex as an efficient catalyst for the epoxidation of alkenes.

### Mechanism studies

Heterogeneous salen and salen-type cobalt complexes have been reported to show catalytic activity for the epoxidation of olefins in the presence of O<sub>2</sub>, although a sacrificial co-reductant, such as isobutyraldehyde [11] or DMF as a solvent and co-reductant [31], was necessary.

For elucidation of the sacrificial co-reductant activity of the catalyst (substrate), we prepared the monomeric analogue of the catalyst and performed the epoxidation reaction under the same conditions as described for the epoxidation of cyclohexene in Table 3. As shown at Scheme 2, *N*-salicylidene-*o*-aminophenol showed that the reaction of 2-aminophenol with salicylaldehyde was prepared with the previously described procedure [52], and complexed to Co and used as a catalyst for the epoxidation of cyclohexene in optimum conditions (cyclohexene (10 mmol), catalyst 5 (50 mg), 60 °C, CH<sub>3</sub>CN (20 mL), O<sub>2</sub> (~1 atm., bubbling 15 mL/min), 4.2 h).



**Scheme 2** Preparation of *N*-salicylidene-*o*-aminophenol (saphH2)

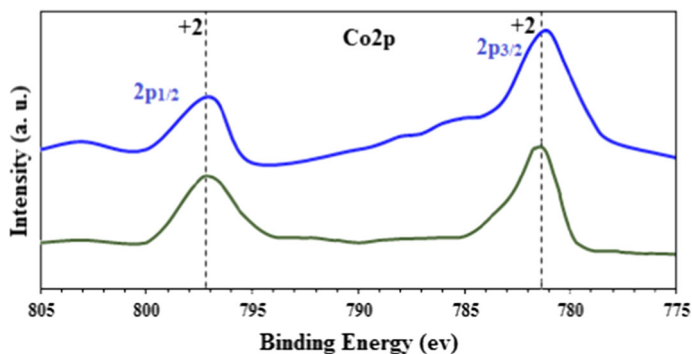


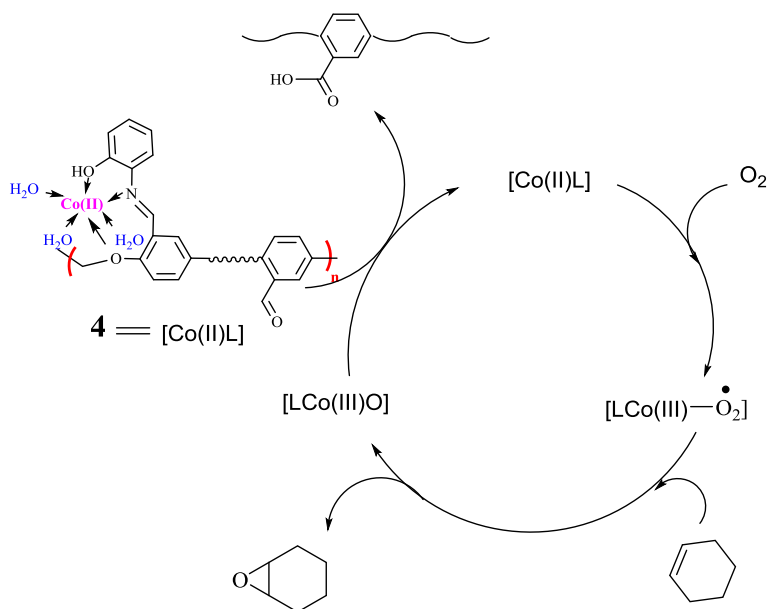
**Fig. 9** XPS spectra of the catalyst (*blue curve*) and the recovered catalyst result in the epoxidation of cyclohexene (*green curve*). (Color figure online)

The results demonstrated just 17% conversion for cyclohexene. It is believed that the absence of any reductant stops the epoxidation cycle. Surprisingly, the addition of the polymeric ligand, PSA **3**, to the reaction mixture caused the progress of the reaction to 56% after 6 h, which was evidence for the effect of the substrate as a sacrificial agent.

Furthermore, in order to be completely sure about the oxidation state of Co in the complex, we used X-ray photoelectron spectroscopy (XPS) analysis. The XPS spectra demonstrated that all the cobalt species in the fresh and recovered catalyst **4** presented in the +2 oxidation state, corresponding to the binding energy of 797 (Co 2p<sub>1/2</sub>) and 781 eV (Co 2p<sub>3/2</sub>) [70–72]. The results clearly proved the sacrificial co-reductant activity of the catalyst **4** which can completely reduce the Co(III) to Co(II) with free aldehyde groups in its framework (Fig. 9).

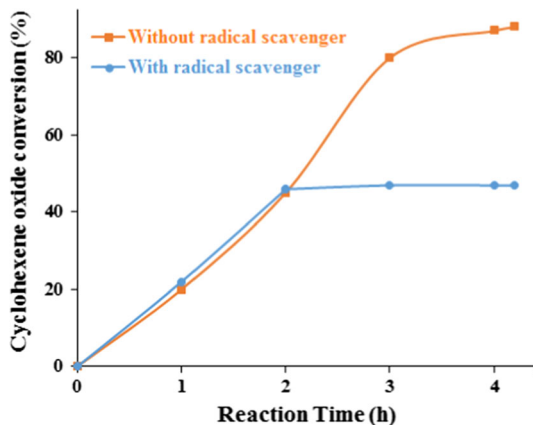
According to the reported mechanisms in the literature for Co complexes catalyzed epoxidation [31, 69, 73] along with our observations, we propose a mechanism for the PSA–Schiff base Co(II) complex-catalyzed epoxidation of alkenes (Scheme 3). In this mechanism, the catalyst **4** is assumed to play two roles. First, epoxidation of alkene through Co-superoxo radicals (which are sensitive to radical scavengers) results in the reaction of Co(II) sites with molecular oxygen; second, the presence of the free aldehyde group in the framework of the catalyst **4** causes the reduction of Co(III) to Co(II) species (Scheme 3). The reaction of the catalyst **4** with molecular oxygen gave Co-superoxo species [31, 69, 73]. Epoxidation of the substrate was performed by Co-superoxo species and gave an epoxide product and LCo(III)O. species. Then, the reduction of Co(III) to Co(II) species occurred by the oxidation of free aldehyde groups on the catalyst **4**. This mechanism explains both the presence of the Co(II) and Co(III) sites in the catalyst in the reaction mixture and the role of the substrate as an activating agent for the reduction of Co(III) to Co(II) species.

In order to demonstrate the presence of radical species (LCo(III)-O.) in our reactions, hydroquinone, as a radical scavenger, was added after 2 h of the reaction, and the reaction progress was monitored by GC. It was observed that the reaction stopped immediately upon addition of the radical scavenger (Fig. 10, blue curve),



**Scheme 3** Proposed mechanism for PSA-Schiff base Co(II) complex

**Fig. 10** Comparison between reactions with hydroquinone as a radical scavenger (blue curve) and a control reaction without adding a radical scavenger (orange curve). (Color figure online)



which suggests that the process indeed proceeds via formation of LCo(III)-O<sub>2</sub> species.

To test the worth of the present work, we comprised our catalyst with some of the reported catalysts in the literature for the epoxidation of cyclooctene (Table 4). Cyclooctene oxide was formed by the PSA-Schiff base Co(II) complex in a short reaction time in CH<sub>3</sub>CN at 60 °C.

Also, the advantage of the present method is that epoxidation occurred by a heterogeneous Co(II) catalyst without the need for an external co-reductant in mild conditions by using O<sub>2</sub> as a green oxidant in short reaction times. It uses a readily

**Table 4** Comparison of catalytic activity of the present catalyst with the other reported catalysts for the epoxidation of cyclooctene

Entry	Catalyst	Conditions	Time (h)	Epoxide yield (%)	References
1	POMs-MOF	CH <sub>3</sub> CN/H <sub>2</sub> O <sub>2</sub> /50 °C	5	82	[3]
2	Amberlite-HCO <sub>3</sub>	CH <sub>3</sub> CN/anisole/H <sub>2</sub> O <sub>2</sub> /r.t	24	75	[74]
3	Cobalt(II)-exchanged zeolite X	DMF/O <sub>2</sub> /100 °C	8	47	[11]
4	Cobalt(III) Schiff base complex	CH <sub>3</sub> CN/isobutyraldehyde/air/60 °C	8	92	[69]
5	Co(II)-exchanged SAPO-34	DMF/H <sub>2</sub> O <sub>2</sub> /air/100 °C	6	11	[75]
6	Ti-LHMS-3	CH <sub>3</sub> CN/TBHP/Reflux	22	68	[76]
7	MnO	DMF/NaHCO <sub>3</sub> /H <sub>2</sub> O <sub>2</sub> /r.t	5	19	[77]
8	Co(ac) <sub>2</sub> ·4H <sub>2</sub> O	CH <sub>3</sub> CN/isobutyraldehyde/air/60 °C	8	24	[78]
9	Co(acac) <sub>3</sub>	CH <sub>3</sub> CN/isobutyraldehyde/air/60 °C	8	25	[78]
10	PSA-Schiff base Co(II) complex	CH <sub>3</sub> CN/O <sub>2</sub> /60 °C	3	90	Present work

available, safe and environmental friendly material for the preparation of the catalyst. High selectivity, no tedious work-up and no by-product are other advantages of the method. Furthermore, a comparison of the catalytic efficiency of **4** with other cobalt salts (cobalt(II) acetate and cobalt(III) acetylacetonate) in a homogeneous medium (Table 4, entries 9, 10) clearly indicates that the PSA-Schiff base Co(II) complex performs as a more efficient reusable catalyst than simple cobalt salts.

## Conclusion

The PSA-Schiff base-Co(II) complex was synthesized through a simple procedure, and cheap and commercially accessible organic material which can catalyze the epoxidation of various olefins through a free co-reductant protocol in the presence of molecular oxygen. The catalyst was characterized with FTIR, UV-Vis, <sup>1</sup>H NMR, CHN, ICP-OES, XPS, EDX and TGA instruments. Average molecular weight of PSA was found to be 2278. The method demonstrated good chemoselectivity toward terminal and on-conjugated olefins. Furthermore, the catalyst can be simply recovered from the reaction mixture and reused for 5 runs without any notable reactivity, selectivity and efficiency loss.

**Acknowledgement** The authors are grateful to Golestan University research council for financial support of this work.

## References

1. F. Ullmann, W. Gerhartz, Y.S. Yamamoto, R. Campbell, F.T. Pfeifferkorn, J.F. Rounsaville Ullmanns, *Encyclopedia of Industrial Chemistry*, vol. 1 (Wiley, Weinheim, 2003)
2. B. Qi, X.H. Lu, D. Zhou, Q.H. Xia, Z.R. Tang, S.Y. Fang, T. Pang, Y.L. Dong, *J. Mol. Catal. A: Chem.* **322**, 73 (2010)
3. H. Haddadi, S.M. Hafshejani, M.R. Farsani, A.K. Babahydari, *New J. Chem.* **39**, 9879 (2015)
4. F. Loeker, W. Leitner, *Chem. Eur. J.* **6**, 2011 (2000)
5. J.M. Brégeault, *Dalton Trans.* **17**, 3289 (2003)
6. E. Angelescu, R. Ionescu, O.D. Pavel, R. Zavoianu, R. Birjega, C.R. Luculescu, M. Florea, R. Olar, *J. Mol. Catal. A: Chem.* **315**, 178 (2010)
7. M.V. Patil, M.K. Yadav, R.V. Jasra, *J. Mol. Catal. A: Chem.* **277**, 72 (2007)
8. M. Lakshmi Kantam, B. Purna Chandra Rao, R. Sudarshan Reddy, N.S. Sekhar, B. Sreedhar, B.M. Choudary, *J. Mol. Catal. A: Chem.* **272**, 1 (2007)
9. X. Zhang, C. Zeng, L. Zhang, N. Xu, *Kinet. Catal.* **50**, 199 (2009)
10. X.H. Lu, Q.H. Xia, S.Y. Fang, B. Xie, B. Qi, Z.R. Tang, *Catal. Lett.* **131**, 517 (2009)
11. K.M. Jinka, J. Sebastian, R.V. Jasra, *J. Mol. Catal. A: Chem.* **274**, 33 (2007)
12. X.Y. Quek, Q. Tang, S. Hu, Y. Yang, *Appl. Catal. A* **361**, 130 (2009)
13. K.J. Balkus, A.K. Khanmamedova, K.M. Dixon, F. Bedioui, *Appl. Catal. A Gen.* **143**, 159 (1996)
14. S. Iffet, G. Necla, G. Turgut, *Synth. React. Inorg. Met. Org. Chem.* **31**, 1175 (2001)
15. M. Salavati-Niasari, M. Shakouri-Arani, F. Davar, *Microporous Mesoporous Mater.* **116**, 77 (2008)
16. V. Ayala, A. Corma, M. Iglesias, J.A. Rincon, F. Sanchez, *J. Catal.* **224**, 170 (2004)
17. A.R. Silva, V. Budarin, J.H. Clark, B. De Castro, C. Freire, *Carbon* **43**, 2096 (2005)
18. M. Turner, V.B. Golovko, O.P.H. Vaughan, P. Abdulkin, A. Berenguer-Murcia, M.S. Tikhov, B.F.G. Johnson, R.M. Lambert, *Nature* **454**, 981 (2008)
19. T. Sreethawong, Y. Yamada, T. Kobayashi, S. Yoshikawa, *J. Mol. Catal. A: Chem.* **241**, 23 (2005)
20. F. Farzaneh, E. Zamanifar, C.D. Williams, *J. Mol. Catal. A* **218**, 203 (2004)
21. O. Cussó, I. Garcia-Bosch, X. Ribas, J. Lioret-Fillol, M. Costas, *J. Am. Chem. Soc.* **135**, 14871 (2013)
22. Y. Zhang, J. Zhao, L. He, D. Zhao, S. Zhang, *Microporous Mesoporous Mater.* **94**, 159 (2006)
23. F.P. Ballistreri, C.M.A. Gangemi, A. Pappalardo, G.A. Tomaselli, R.M. Toscano, G. Trusso Sfrassetto, *Int. J. Mol. Sci.* **17**, 1112 (2016)
24. T. Yamada, T. Takai, O. Rhode, T. Mukaiyama, *Chem. Lett.* **1**, 1 (1991)
25. C. Zeng, D. Yuan, B. Zhao, Y. Yao, *Org. Lett.* **17**, 2242 (2015)
26. C. Wang, H. Yamamoto, *J. Am. Chem. Soc.* **136**, 1222 (2014)
27. K.A. Jørgensen, *Chem. Rev.* **89**, 431 (1989)
28. R. Hunter, P. Turner, S. Rimmer, *Synth. Commun.* **30**, 4461 (2000)
29. M. Salavati-Niasari, E. Esmacili, H. Seyghalkar, M. Bazarganipour, *Inorg. Chim. Acta* **375**, 11 (2011)
30. Y.L. Hu, Y.W. Liu, D.J. Li, *J. Iran. Chem. Soc.* **12**, 2179 (2015)
31. M.J. Beier, W. Kleist, M.T. Wharmby, R. Kissner, B. Kimmerle, P.A. Wright, J.D. Grunwaldt, A. Baiker, *Chem. Eur. J.* **18**, 887 (2012)
32. Q.H. Tang, Q.H. Zhang, H.L. Wu, Y. Wang, *J. Catal.* **230**, 384 (2005)
33. R. Raja, G. Sankar, J.M. Thomas, *Chem. Commun.* 829 (1999)
34. D. Dhar, Y. Kolytyn, A. Gedanken, S. Chandrasekaran, *Catal. Lett.* **86**, 197 (2003)
35. T. Pruß, D.J. Macquarrie, J.H. Clark, *Appl. Catal. A Gen.* **276**, 29 (2004)
36. Z. Opre, T. Mallat, A. Baiker, *J. Catal.* **245**, 482 (2007)
37. X.J. Meng, K.F. Lin, X.Y. Yang, Z.H. Sun, D.Z. Jiang, F.S. Xiao, *J. Catal.* **218**, 460 (2003)
38. S.L. Pandhare, R.R. Jadhav, V.G. Puranik, P.V. Joshi, F. Capet, M.K. Dongare, S.B. Umbarkar, C. Michon, *J. Organomet. Chem.* **772**, 271 (2014)
39. A.C. Gomes, S.M. Bruno, M. Abrantes, C.I.R. Magalhães, I.S. Gonçalves, A.A. Valente, M. Pillinger, *J. Organomet. Chem.* **760**, 205 (2014)
40. E. Stochmal-Pomarzanska, M. Hasik, W. Turek, A. Pron, *J. Mol. Catal. A: Chem.* **114**, 267 (1996)
41. T. Punniyamurthy, S. Velusamy, J. Iqbal, *Chem. Rev.* **105**, 2329 (2005)
42. B.C. Das, J. Iqbal, *Tetrahedron Lett.* **38**, 2903–2906 (1997)
43. A.J. Butterworth, J.H. Clark, P.H. Walton, S.J. Barlow, *Chem. Commun.* **16**, 1859 (1996)

44. B.B. Wentzel, S.M. Leinonen, S. Thomson, D.C. Sherrington, M.C. Feiters, R.J.M. Nolte, *J. Chem. Soc. Perkin Trans. I* **20**, 3428 (2000)
45. W. Naqash, K. Majid, *Mater. Res.* **18**, 1121 (2015)
46. A.S. Goldstein, R.H. Beer, R.S. Drago, *J. Am. Chem. Soc.* **116**, 2424 (1994)
47. K.M. Jinka, S.M. Pai, B.L. Newalkar, N.V. Choudary, R.V. Jasra, *Catal. Commun.* **11**, 638 (2010)
48. X.H. Lu, Q.H. Xia, D. Zhou, S.Y. Fang, Y.L. Dong, *Catal. Commun.* **11**, 106 (2009)
49. C.I. Fernandes, M.D. Carvalho, L.P. Ferreira, C.D. Nunes, P.D. Vaz, *J. Organomet. Chem.* **760**, 2 (2014)
50. Q. Tang, Y. Wang, J. Liang, P. Wang, Q. Zhang, H. Wan, *Chem. Commun.* 440 (2004)
51. Y. Nishiyama, Y. Nakagawa, N. Mizuno, *Angew. Chem. Int. Ed.* **40**, 3639 (2001)
52. M.S. Refat, M.Y. El-Sayed, A.M.A. Adam, *J. Mol. Struct.* **1038**, 62 (2013)
53. M.D. Hughes, Y.J. Xu, P. Jenkins, P. McMorn, P. Landon, D.I. Enache, A.F. Carley, G.A. Attard, G.J. Hutchings, F. King, E.H. Stitt, P. Johnston, K. Griffin, C.J. Kiely, *Nature* **437**, 1132 (2005)
54. A.K. Sinha, S. Seelan, S. Tsubota, M. Haruta, *Angew. Chem. Int. Ed.* **43**, 1546 (2004)
55. I. Yamanaka, M. Soma, K. Oisuka, *J. Chem. Soc., Chem. Commun.* 2235 (1995)
56. R. Ben-Daniel, L. Weiner, R. Neumann, *J. Am. Chem. Soc.* **124**, 8788 (2002)
57. X. Wang, Q. Zhang, Q. Guo, Y. Lou, L. Yang, Y. Wang, *Chem. Commun.* 1396 (2004)
58. D. Janes, S. Kreft, *Food Chem.* **109**, 293 (2008)
59. R. Tang, F.X. Webster, D. Müller-Schwarze, *J. Chem. Ecol.* **19**, 1491 (1993)
60. Q. Wang, C. Wilson, A.J. Blake, S.R. Collinson, P.A. Tasker, M. Schröder, *Tetrahedron Lett.* **47**, 8983 (2006)
61. M. Pramanik, S.K. Mendon, J.W. Rawlins, *Polym. Test* **31**, 716 (2012)
62. V.P. Boiko, V.K. Grischenko, *Acta Polym.* **36**, 459 (1985)
63. J.F. Zemaits Jr., D.M. Clark, M. Rafal, N.C. Scrivner, *Handbook of Aqueous Electrolyte Thermodynamics: Theory and Application* (Wiley, New Jersey, 1986)
64. X.H. Lu, Q.H. Xia, H.J. Zhan, H.X. Yuan, C.P. Ye, K.X. Su, G. Xu, *J. Mol. Catal. A: Chem.* **250**, 62 (2006)
65. N. Nishat, S. Hasnain, T. Ahmad, A. Parween, J. Therm. Anal. Calorim. **105**, 969 (2011)
66. Y. Pérez, S. Bázquez, M. Fajardo, P. De Frutos, I. Del Hierro, *J. Organomet. Chem.* **741**, 102 (2013)
67. A.A.A. Aziz, A.N.M. Salem, M.A. Sayed, M.M. Aboaly, *J. Mol. Struct.* **1010**, 130 (2012)
68. G. Maayan, R. Neumann, *Chem. Commun.* 4595 (2005)
69. D. Saha, T. Maity, R. Bera, S. Koner, *Polyhedron* **56**, 230 (2013)
70. X. Li, S. Yang, J. Sun, P. He, X. Pu, G. Ding, *Synth. Met.* **194**, 52 (2014)
71. A. Indra, P.W. Menezes, C. Das, C. Göbel, M. Tallarida, D. Schmeißer, M. Driess, *J. Mater. Chem. A Mater. Energy Sustain.* **5**, 5171 (2017)
72. C. Oh, D. Choo, W. Shim, D. Lee, E. Roh, C. Song, *Chem. Commun.* 1100 (2003)
73. P. Buranaprasertsuk, Y. Tangsakol, W. Chavasiri, *Catal. Commun.* **8**, 310 (2007)
74. J. Mielby, S. Kegnæs, *Catal. Lett.* **143**, 1162 (2013)
75. B. Tang, X.H. Lu, D. Zhou, P. Tian, Z.H. Niu, J.-L. Zhang, X. Chen, Q.H. Xia, *Catal. Commun.* **31**, 42 (2013)
76. A. Modak, M. Nandi, A. Bhaumik, *Catal. Today* **198**, 45 (2012)
77. B. Qi, L.L. Lou, K. Yu, W. Bian, S. Liu, *Catal. Commun.* **15**, 52 (2011)
78. D. Saha, T. Maity, R. Bera, S. Koner, *Polyhedron* **56**, 230 (2013)